

2002

Vanadate-Induced Expression Of Hypoxia-Inducible Factor 1A And Vascular Endothelial Growth Factor Through Phosphatidylinositol 3-Kinase/Akt Pathway And Reactive Oxygen Species

Ning Gao

Min Ding

Jenny Z. Zheng

Zhuo Zhang

Stephen S. Leonard

See next page for additional authors

Follow this and additional works at: https://researchrepository.wvu.edu/faculty_publications

Digital Commons Citation

Gao, Ning; Ding, Min; Zheng, Jenny Z.; Zhang, Zhuo; Leonard, Stephen S.; Liu, Ke Jian; Shi, Xianglin; and Jiang, Bing-Hua, "Vanadate-Induced Expression Of Hypoxia-Inducible Factor 1A And Vascular Endothelial Growth Factor Through Phosphatidylinositol 3-Kinase/Akt Pathway And Reactive Oxygen Species" (2002). *Faculty Scholarship*. 725.
https://researchrepository.wvu.edu/faculty_publications/725

Authors

Ning Gao, Min Ding, Jenny Z. Zheng, Zhuo Zhang, Stephen S. Leonard, Ke Jian Liu, Xianglin Shi, and Bing-Hua Jiang

Vanadate-induced Expression of Hypoxia-inducible Factor 1 α and Vascular Endothelial Growth Factor through Phosphatidylinositol 3-Kinase/Akt Pathway and Reactive Oxygen Species*

Received for publication, January 3, 2002, and in revised form, April 16, 2002
Published, JBC Papers in Press, June 17, 2002, DOI 10.1074/jbc.M200082200

Ning Gao \ddagger , Min Ding \S , Jenny Z. Zheng \ddagger , Zhuo Zhang \S , Stephen S. Leonard \S , Ke Jian Liu \parallel ,
Xianglin Shi \S , and Bing-Hua Jiang $\ddagger\parallel$

From the \ddagger Mary Babb Randolph Cancer Center, Department of Microbiology, Immunology and Cell Biology, West Virginia University, Morgantown, West Virginia 26506-9300, the \S Health Effects Laboratory Division, National Institute for Occupational Safety and Health, Morgantown, West Virginia 26505, and the \parallel College of Pharmacy, University of New Mexico, Albuquerque, New Mexico 87131

Hypoxia-inducible factor 1 (HIF-1) is a heterodimeric basic helix-loop-helix transcription factor composed of HIF-1 α and HIF-1 β /aryl hydrocarbon nuclear translocator subunits. HIF-1 expression is induced by hypoxia, growth factors, and activation of oncogenes. In response to hypoxia, HIF-1 activates the expression of many genes including vascular endothelial growth factor (VEGF) and erythropoietin. HIF-1 and VEGF play an important role in angiogenesis and tumor progression. Vanadate is widely used in industry, and is a potent inducer of tumors in humans and animals. In this study, we demonstrate that vanadate induces HIF-1 activity through the expression of HIF-1 α but not HIF-1 β subunit, and increases VEGF expression in DU145 human prostate carcinoma cells. We also studied the signaling pathway involved in vanadate-induced HIF-1 α and VEGF expression and found that phosphatidylinositol 3-kinase/Akt signaling was required for HIF-1 and VEGF expression induced by vanadate, whereas mitogen-activated protein kinase pathway was not required. We also found that reactive oxygen species (ROS) were involved in vanadate-induced expression of HIF-1 and VEGF in DU145 cells. The major species of ROS responsible for the induction of HIF-1 and VEGF expression was H₂O₂. These results suggest that the expression of HIF-1 and VEGF induced by vanadate through PI3K/Akt may be an important signaling pathway in the vanadate-induced carcinogenesis, and ROS may play an important role.

Hypoxia-inducible factor 1 (HIF-1)¹ is a heterodimer of HIF-1 α and HIF-1 β subunits, which contain basic helix-loop-helix PAS domains (1, 2). HIF-1 α is a unique subunit tightly

regulated in response to hypoxia (2, 3), whereas HIF-1 β is identical to the aryl hydrocarbon nuclear translocator that forms heterodimers with the aryl hydrocarbon receptor in cells (2, 4). HIF-1 regulates the expression of many genes including vascular endothelial growth factor (VEGF), erythropoietin, heme oxygenase 1, aldolase, enolase, and lactate dehydrogenase A (5–8). The levels of HIF-1 activity in cells correlate with tumorigenicity and angiogenesis in nude mice (9, 10). HIF-1 is also induced by the expression of oncogenes such as v-Src and Ras (9, 11), and is overexpressed in many human cancers (12). Recent studies indicate that both phosphatidylinositol 3-kinase (PI3K)/Akt and MAP kinase pathway are involved in HIF-1 expression induced by growth factors (13–16). HIF-1 α interacts with tumor suppressor Von Hippel-Lindau protein. The mutation of Von Hippel-Lindau protein in human cancers results in the constitutive expression of HIF-1 under nonhypoxic conditions (17). HIF-1 α is degraded by the proteasome pathway (18–21). The regulation of HIF-1 by Von Hippel-Lindau protein and cellular oxygen was recently shown to be mediated through the prolyl hydroxylation of HIF-1 α at Pro⁵⁶⁴ by three mammalian PHDs proteins (22–24). One of the major genes regulated by HIF-1 is VEGF (5, 25). VEGF plays a key role in tumor progression and angiogenesis. There is a strong correlation between VEGF expression and blood vessel density in many tumor types (26). Inhibition of VEGF expression and of its receptor function dramatically decreases the tumor growth, invasion, and metastasis in animal models (27–30). Somatic mutations such as oncogene Ras activation and tumor suppressor gene p53 inactivation also increase VEGF expression (26).

Vanadium is a widely distributed trace metal. The burning of fossil fuels (petroleum, coal, and oil) in power and heat producing plants causes widespread discharge of vanadium into the environment (31, 32). Vanadium exists in oxidation states ranging from –1 to +5. Among these oxidation states, the pentavalent state is the most stable form. Previous studies provide evidence that in mammalian systems vanadium(V) is more toxic than vanadium(IV). The data on the carcinogenic activity of vanadium is limited. Epidemiological studies have shown a correlation between vanadium exposure and the incidence of cancer in humans (33–36). Some reports indicate that vanadium increases the frequency of micronuclei and polyploid cells, decreases mitotic index, and induces DNA single strand breaks and DNA-protein cross-links (37–39). Previous *in vitro* studies using cultured mouse embryo fibroblast BALB/3T3 cells and the Syrian hamster embryo cells demonstrated that this metal is a carcinogen (40–43). Although the mechanisms of vanadate-induced carcinogenesis are not fully understood,

* This work was supported by National Institutes of Health NCI Grant RR16440 and American Heart Association Grant 0160166B (to B. H. J.). The costs of publication of this article were defrayed in part by the payment of page charges. This article must therefore be hereby marked "advertisement" in accordance with 18 U.S.C. Section 1734 solely to indicate this fact.

\parallel To whom correspondence should be addressed. Tel.: 304-293-5949; Fax: 304-293-4667; E-mail: bhjiang@hsc.wvu.edu.

¹ The abbreviations used are: HIF-1, hypoxia-inducible factor 1; VEGF, vascular endothelial growth factor; ROS, reactive oxygen species; ARNT, aryl hydrocarbon nuclear translocator; PI3K, phosphatidylinositol 3-kinase; MAP kinase, mitogen-activated protein kinase; MEK, mitogen-activated protein kinase kinase; mTOR, mammalian target of rapamycin; MEM, minimum essential medium; DPI, diphenylene iodonium; FBS, fetal bovine serum; PBS, phosphate-buffered saline; ELISA, enzyme-linked immunosorbent assay; HE, dihydroethidium; DMPD, 5,5-dimethyl-1-pyrroline-1-oxide.

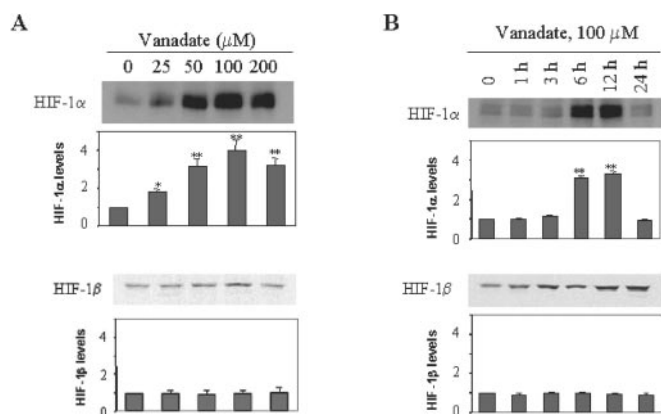


FIG. 1. Induction of HIF-1 expression by vanadate. A, DU145 cells were treated without (lane 1) or with 25–200 μM vanadate (lanes 2–5) for 6 h. B, DU145 cells were treated without (lane 1) and with 100 μM vanadate for 1, 3, 6, 12, and 24 h, respectively. Cellular extracts were prepared and subjected to immunoblot assay using an anti-HIF-1 α monoclonal antibody. The blot was then stripped and detected for HIF-1 β expression using antibodies against HIF-1 β . The immunoblot signals were quantified using molecular analyst/PC densitometry software (Bio-Rad). The mean densitometry data from independent experiments (one of which is shown here) were normalized to the result obtained in cells in the absence of vanadate (control). Plots are mean \pm S.E. values ($n = 3$); *, $p < 0.05$ compared with the control; **, $p < 0.01$ compared with the control.

reactive oxygen species (ROS) are considered to play an important role (44, 45). It has been reported that upon reduction by cellular reactants, vanadate is able to generate a whole spectrum of ROS, *i.e.* O_2^- , H_2O_2 , and $\cdot\text{OH}$. It is well known that ROS play an important role in carcinogenesis induced by a variety of carcinogens. Through ROS-mediated reaction, vanadate is able to induce activation of activator protein-1 expression (44, 45). Recent studies have found that vanadium is able to mimic the effect of insulin (46–49). Therefore, we tested whether vanadate is able to induce the expression of HIF-1 α and VEGF in DU145 human prostate carcinoma cells and evaluated the role of individual ROS. The following specific questions were addressed: (a) whether vanadate is able to induce HIF-1 and VEGF expression; (b) which signaling pathway(s) is/are involved in vanadate-induced expression of HIF-1 α protein; (c) whether ROS species are involved in vanadate-induced HIF-1 α and VEGF expression; and (d) which species of ROS play a critical role.

MATERIALS AND METHODS

Reagents and Cell Culture—Sodium orthovanadate, NADPH, superoxide dismutase, sodium formate, deferoxamine, diphenylene iodonium (DPI), and rotenone were purchased from Sigma. Catalase was purchased from Roche Molecular Biochemicals (Indianapolis, IN). Antibodies against HIF-1 α and HIF-1 β were from Transduction Laboratories (Lexington, KY), phospho-Akt (Ser473) and Akt antibodies were from Cellular Signaling (Beverly, MA). The human VEGF immunoassay kit was from R&D Systems (Minneapolis, MN).

The human prostate cancer cell line DU145 was maintained in minimum essential medium (MEM) (Invitrogen) supplemented with 10% fetal bovine serum (FBS), 3% chicken serum, 2 mM L-glutamine, 100 units/ml penicillin, and 100 $\mu\text{g}/\text{ml}$ streptomycin, and cultured at 37 $^\circ\text{C}$ in a 5% CO_2 incubator. The cells form a monolayer at confluence. Trypsin (0.25%)/EDTA solution was used to detach the cells from the culture flask for passing the cells.

Immunoblot Analysis—The cells were plated in a 60-mm culture dish and treated with vanadate. Cells were lysed in RIPA buffer (150 mM NaCl, 100 mM Tris (pH 8.0), 1% Triton X-100, 1% deoxycholic acid, 0.1% SDS, 5 mM EDTA, and 10 mM NaF) supplemented with 1 mM sodium vanadate, 2 mM leupeptin, 2 mM aprotinin, 1 mM phenylmethylsulfonyl fluoride, 1 mM dithiothreitol, and 2 mM pepstatin A on ice for 30 min. After centrifugation at 14,000 rpm for 15 min, the supernatant was harvested as the total cellular protein extracts and stored at -70°C . The protein concentration was determined using Bio-Rad protein assay

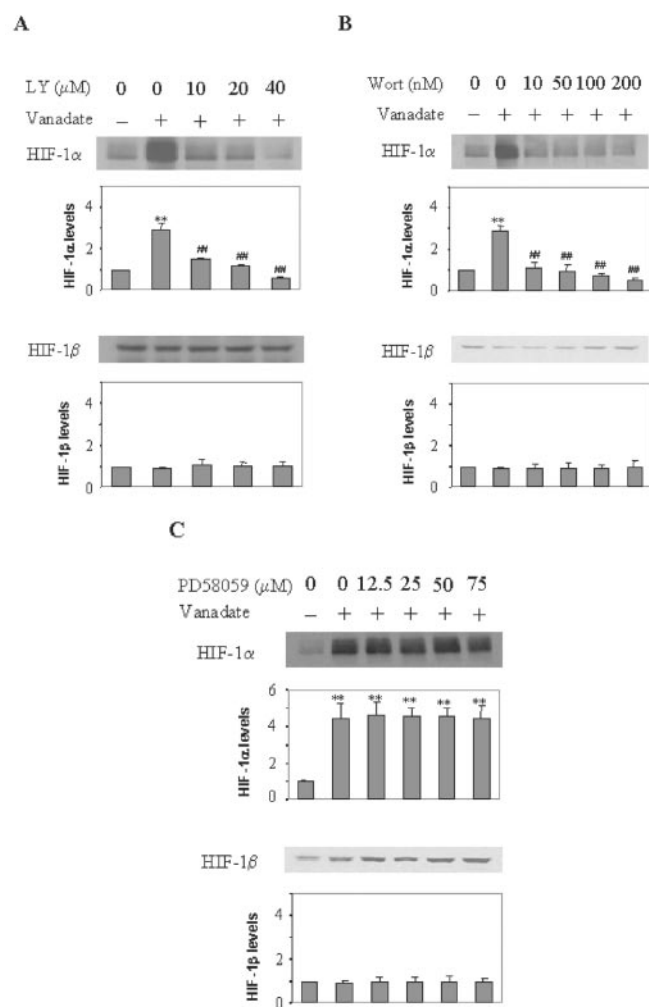


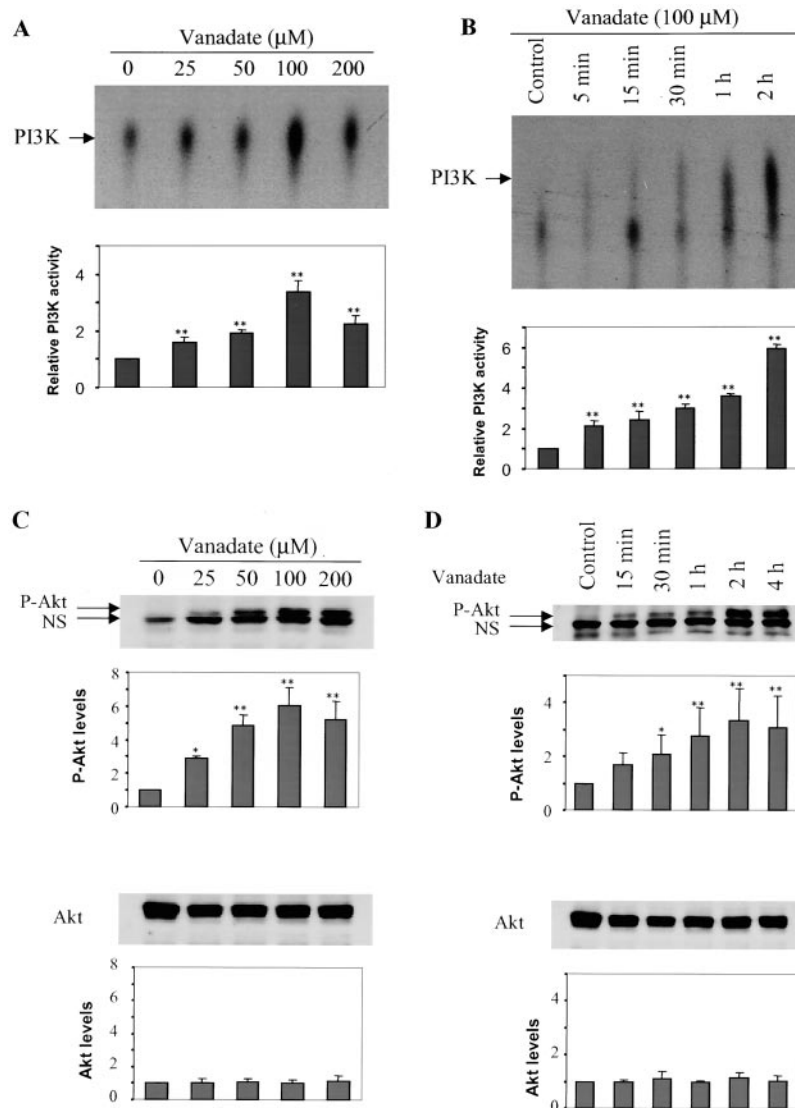
FIG. 2. Effect of pharmacological inhibitors of PI3K and MEK on HIF-1 expression induced by vanadate. DU145 cells were cultured in MEM supplemented with 10% FBS for 24 h at 37 $^\circ\text{C}$ in 5% CO_2 incubator, followed by the addition of LY294002 (A), wortmannin (B), and PD98059 (C) at the concentrations indicated, and incubated for 30 min. Cells were then treated with 100 μM vanadate for an additional 6 h. Cellular lysates were prepared and used for immunoblot assay using antibodies against HIF-1 α and HIF-1 β as indicated. The immunoblot signals were quantitated and analyzed as described in the legend to Fig. 1. Plots are mean \pm S.E. ($n = 3$); **, $p < 0.01$ compared with the control; ##, $p < 0.01$ compared with the values from the cells treated by vanadate in the absence of LY294002 and wortmannin.

reagents. The total cellular protein extracts were separated by SDS-PAGE, and transferred to nitrocellulose membrane in 20 mM Tris-HCl (pH 8.0) containing 150 mM glycine and 20% (v/v) methanol. Membranes were blocked with 5% nonfat dry milk in $1\times$ TBS containing 0.05% Tween 20 and incubated with antibodies against HIF-1 α , HIF-1 β , phospho-Akt (Ser473), and Akt. Protein bands were detected by incubation with horseradish peroxidase-conjugated antibodies (PerkinElmer Life Sciences), and visualized with enhanced chemiluminescence reagent (PerkinElmer Life Sciences).

PI3K Assay—Cells were washed with ice-cold PBS and scraped from the plates, and centrifuged at 4,000 rpm for 5 min. The cell pellet was incubated for 20 min on ice in lysis buffer (150 mM NaCl, 100 mM Tris-HCl (pH 8.0), 1% Triton X-100, 5 mM EDTA, 10 mM NaF) supplemented with 1 mM dithiothreitol, 1 mM phenylmethylsulfonyl fluoride, 1 mM sodium vanadate, 2 mM leupeptin, and 2 mM aprotinin, and centrifuged at $15,000\times g$ for 15 min to clarify the supernatants. PI3K activity was analyzed using 400 μg of protein extracts and anti-p110 antibodies as described (28, 29). Briefly, 400 μg of total protein was incubated with 20 μl of protein A/G plus agarose for 1 h at 4 $^\circ\text{C}$ on a rotator, followed by spinning at 3,000 rpm for 3 min. The supernatant was then incubated with 10 μl of antibodies against p110 subunit of PI3K for 1 h at 4 $^\circ\text{C}$. Protein A/G-agarose beads (30 μl) were added for

FIG. 3. Effect of vanadate on PI3K activity and phosphorylation of Akt.

A, DU145 cells were treated with various concentrations of vanadate for 2 h. B, the cells were treated with 100 μM vanadate for different time periods as indicated. The total protein extracts were prepared and used for determining PI3K activity (A and B). C, the cells were treated with certain concentrations of vanadate for 2 h. D, the cells were exposed to 100 μM vanadate from 0 to 4 h as indicated. The total cellular protein extracts were prepared and subjected to immunoblot assay with antibodies against phospho-Akt (Ser473) and Akt (C and D). The immunoblot signals were quantitated and analyzed as described in the legend to Fig. 1. Plots are mean \pm S.E. ($n = 3$); *, $p < 0.05$ compared with the control; **, $p < 0.01$ compared with the control.



an additional 1 h. The beads were then pelleted and washed sequentially with TNE buffer (containing 20 mM Tris, pH 7.5, 100 mM NaCl, and 1 mM EDTA), five times; and once with 20 mM HEPES. PI3K assays were performed using phosphatidylinositol as substrate in a final volume of 50 μl containing 20 mM HEPES (pH 7.5), 10 mM MgCl₂, 2 μCi of [γ -³²P]ATP, 60 μM ATP, and 0.2 mg/ml sonicated phosphatidylinositol. Reactions were carried out for 15 min at room temperature and extracted by the addition of 80 μl of 1 M HCl and 160 μl of chloroform/methanol (1:1). After centrifugation, the organic phase was evaporated to dryness and separated on a TLC plate. PI3K activity was analyzed by the incorporation of ³²P into phosphorylated lipids, and detected by autoradiography.

Densitometry Analysis—Autoradiographic signals of immunoblot and PI3K activity assays were quantified using molecular analyst/PC densitometry software (Bio-Rad). Mean densitometry data from independent experiments were normalized to result in cells in the control. The data were presented as the mean \pm S.E., and analyzed by the Student's *t* test.

VEGF Assay—DU145 cells were plated in a 6-well plate at a density of 1×10^5 cells/well in MEM and incubated overnight before the cells were subjected to treatment. After treatment, the cell culture media were removed for storage at -80°C . Levels of VEGF protein in the medium were determined by ELISA using a commercial kit (R&D Systems, Minneapolis, MN). Briefly, 200 μl of standards or cell culture supernatant were added to the wells of a microplate that was pre-coated with a monoclonal antibody specific for VEGF and incubated for 2 h at room temperature. After washing away any unbound substances, an enzyme-linked polyclonal antibody against VEGF conjugated to horseradish peroxidase was added to the wells and incubated for 2 h at room temperature. Following a wash, 200 μl of substrate solution was added

to the wells and incubated for 30 min, and then 50 μl of stop solution was added to stop color development. The optical density of each well was determined using a microplate reader at 450 nm. The experiments were repeated twice with two replications per experiment. Mean values from these samples were analyzed.

ESR Measurements—The ESR spin trapping technique with DMPO as the spin trap was used to detect free radical generation. This technique involves the addition-type reaction of a short-lived radical with a diamagnetic compound (spin trap) to form a relative long-lived free radical product (spin adduct), which can be studied by conventional ESR (50). The intensity of the spin adduct signal corresponds to the amount of short-lived radicals trapped, and the hyperfine couplings of the spin adduct were generally characteristic of the original trapped radicals. All ESR measurements were conducted using a Varian E9 ESR spectrometer and a flat cell assembly as described (51, 52). Hyperfine couplings were measured (to 0.1 G) directly from magnetic field separation using potassium tetraperoxochromate (K₃CrO₈) and 1,1-diphenyl-2-picrylhydrazyl as reference standards. Reactants were mixed in test tubes in a total final volume of 500 μl and transferred to a flat cell for ESR measurement.

Measurements of Cellular Hydrogen Peroxide (H₂O₂)—Cellular H₂O₂ was determined using a quantitative H₂O₂ assay kit (BIOXYTECH, Portland, OR). The assay was performed according to the protocol provided by the manufacturer. This assay is based on the oxidation of ferrous ions (Fe²⁺) to ferric ions (Fe³⁺) by H₂O₂ under acidic conditions. The ferric ion binds with the indicator dye xylenol orange to form a stable colored complex that can be measured at 560 nm. Briefly, cells were pretreated with vanadate and with or without antioxidants. The aliquots of media were incubated at 25 $^\circ\text{C}$ for 30 min with 100 μl of a 10 \times xylenol orange stock solution (xylenol orange (10 μM),

FIG. 4. Effect of PI3K inhibitors on PI3K activity and Akt phosphorylation. DU145 cells were cultured in MEM supplemented with 10% FBS for 24 h at 37 °C in a 5% CO₂ incubator, followed by pretreatment with LY294002 or wortmannin for 30 min as indicated. The cells were then treated with 100 μM vanadate for an additional 2 h. **A**, the total cellular protein extracts were prepared and used for determining PI3K activity (A). The cells were incubated with LY294002 (**B**) or wortmannin (**C**) for 30 min, followed by treatment with 100 μM vanadate for 2 h. The total cellular protein extracts were prepared and subjected to immunoblot assay with antibodies against phospho-Akt (Ser473) and Akt (**D** and **C**). The immunoblot signals were quantified and analyzed. Plots are mean ± S.E. values ($n = 3$); **, $p < 0.01$ compared with the control; ##, $p < 0.01$ compared with the values from the cells treated by vanadate in the absence of inhibitors.

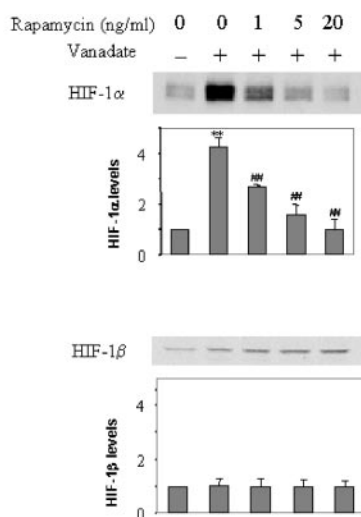
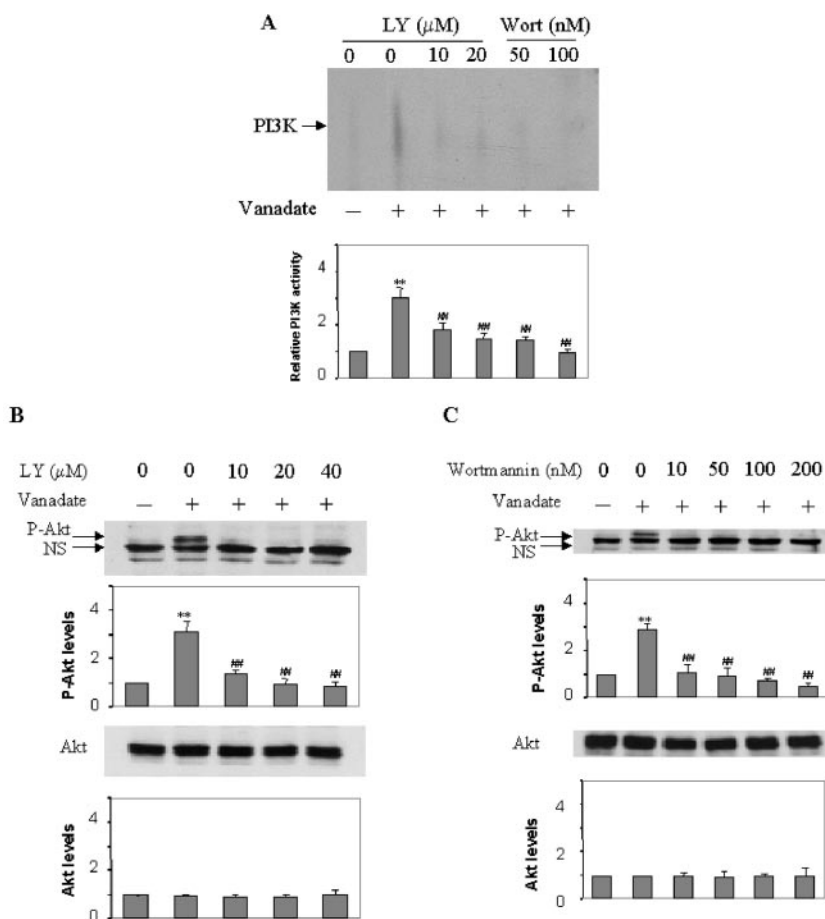


FIG. 5. Effect of rapamycin on HIF-1 expression induced by vanadate. DU145 cells were cultured in MEM supplemented with 10% FBS for 24 h at 37 °C in a 5% CO₂ incubator. The cells were incubated with a mTOR/FRAP inhibitor, rapamycin, at the concentrations indicated for 30 min, followed by treatment with 100 μM vanadate for 6 h. Cellular lysates were prepared and used for immunoblot assay using antibodies against HIF-1α and HIF-1β. The immunoblot signals were quantitated and analyzed. Mean ± S.E. ($n = 3$) are shown. **, $p < 0.01$ compared with the control; ##, $p < 0.01$ compared with the values from the cells treated by vanadate in the absence of rapamycin.

Fe(NH₄)₂(SO₄)·6H₂O (2.5 μM), H₂SO₄ (25 mM)) after which the absorbance was read at 560 nm. The concentration of H₂O₂ was determined from a standard curve.

Superoxide Anion (O₂⁻) Assay—Dihydroethidium (HE) is a specific dye for O₂⁻. HE was oxidized by O₂⁻ to ethidium that stains nucleus to

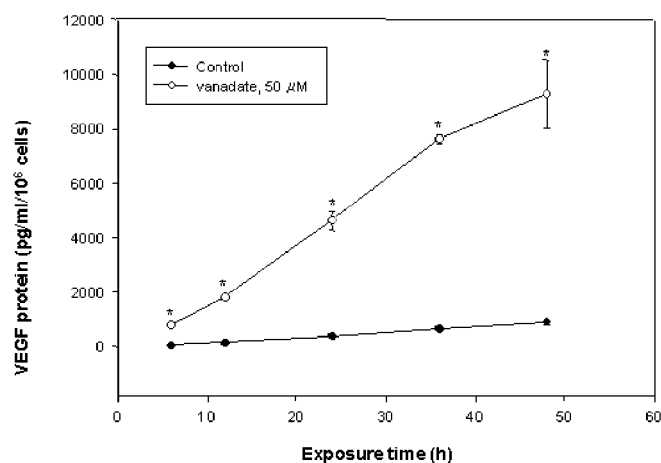


FIG. 6. VEGF protein secretion by DU145 cells treated with vanadate. DU145 cells were seeded in a 6-well plate at a density of 1×10^6 cells/well in MEM supplemented with 10% FBS and incubated for 24 h at 37 °C in a 5% CO₂ incubator. The cells were treated without (●) and with 50 μM vanadate (○) for different time periods as indicated. The concentrations of VEGF protein in the culture media were determined by ELISA. The results represent the mean values of VEGF concentrations from duplicate samples of each experiment and three separate experiments. The asterisk (*) indicates the levels of VEGF significantly increased compared with the control ($p < 0.01$).

form a bright fluorescent red (53). The cells were plated onto a glass coverslip in the 12-well plate at 1×10^5 cells/well 24 h before treatment. HE was added into the cell culture 30 min before vanadate treatment was completed. After being stained, the cells were washed in PBS and fixed with 10% buffered formalin. The coverslip was mounted on a glass slide and observed using a Saratog 2000 (Amersham Biosciences) laser scanning confocal microscope (Optiphot-2, Nikon, Inc., Melville, PA) fitted with an argon-ion laser.

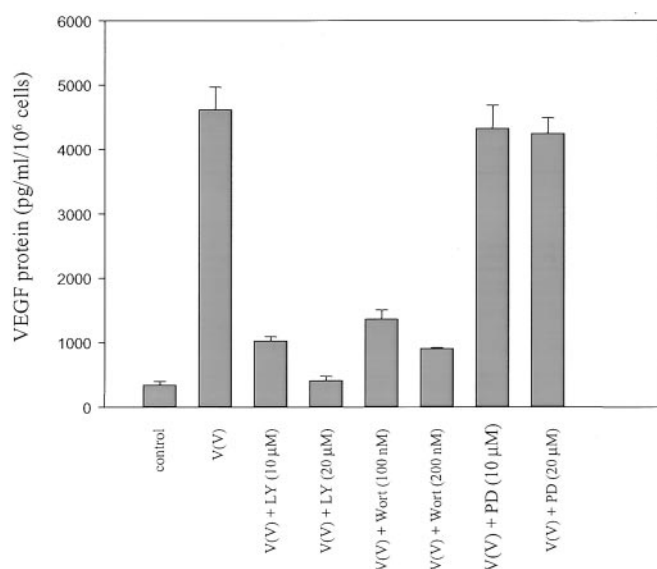


FIG. 7. Effect of inhibitors of PI3K and MEK on VEGF expression induced by vanadate. DU145 cells were seeded in a 6-well plate at a density of 1×10^6 cells/well in MEM supplemented with 10% FBS and incubated for 24 h at 37 °C in a 5% CO₂ incubator, followed by pretreatment with PI 3-kinase inhibitors, LY294002 (10 and 40 μM) and wortmannin (50 and 200 nM), or the MEK inhibitor, PD98059 (25 and 50 μM). Cells were then treated with 50 μM vanadate(V) for 24 h. VEGF protein concentrations in the culture media were determined by ELISA. The results represent the mean values of VEGF concentrations from three separate experiments with duplicate samples of each experiment.

Oxygen Consumption Measurements—Oxygen consumption measurements were carried out with a Gilson oxygraph equipped with a Clark electrode (Gilson Medical Electronic, Middleton, WI). These measurements were made from a mixture containing 1×10^6 cells/ml and various treatments in a total volume of 1.5 ml. The oxygraph was calibrated with media equilibrated with oxygen of known concentrations.

RESULTS

Vanadate Induces HIF-1 Expression—To determine whether vanadate could induce HIF-1 expression, DU145 cells were treated with various concentrations of vanadate for 6 h, and the total cellular protein extracts were prepared for immunoblot assays of HIF-1α and HIF-1β protein levels. As shown in Fig. 1A, levels of HIF-1α protein were induced by vanadate in a dose-dependent manner, whereas the levels of HIF-1β protein were not altered. The maximum expression of HIF-1α was induced by 100 μM vanadate (Fig. 1A). To determine the kinetics of HIF-1α expression induced by vanadate, cells were treated with 100 μM vanadate for various times as indicated, and cellular protein extracts were prepared for analysis of HIF-1α and HIF-1β protein levels. As shown in Fig. 1B, vanadate-induced HIF-1α expression in a time-dependent manner, whereas it did not alter HIF-1β expression. The maximum induction of HIF-1α expression was at 6 h after the treatment. The prolonged exposure of cells to vanadate resulted in the decrease of HIF-1α protein levels, possibly because of the apoptosis of the cells induced by this metal (data not shown).

PI3K but Not Mitogen-activated Protein Kinase/ERK Is Required in Vanadate-induced HIF-1α Expression—To determine whether the PI3K signaling pathway was required for HIF-1α expression induced by vanadate, DU145 cells were pretreated with PI3K inhibitors, LY294002 and wortmannin. The cells were then exposed to vanadate for 6 h, and total cellular protein extracts were prepared for immunoblot assays of HIF-1α and HIF-1β protein levels. As shown in Fig. 2, A and B, PI3K inhibitors, LY294002 and wortmannin, were able to inhibit vanadate-induced HIF-1α expression in a dose-dependent manner, whereas these inhibitors did not change HIF-1β protein

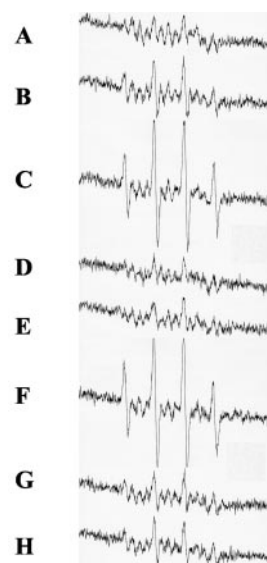


FIG. 8. Effects of antioxidants on vanadate(V)-induced ROS generation. 1×10^6 cells were incubated in PBS containing 100 mM DMPO and 1 mM vanadate(V) with or without antioxidants, DPI and rotenone. ESR spectra were recorded for 30 min. A, DU145 cells only; B, cells + vanadate; C, cells + vanadate + superoxide dismutase (1000 units/ml); D, cells + vanadate + catalase (5,000 units/ml); E, cells + vanadate + sodium formate (2 mM); F, cells + vanadate + NADPH (1 mM); G, cells + vanadate + DPI (20 μM); H, cells + vanadate + rotenone (50 μM).

TABLE I

Relative free radical generation from cells stimulated by vanadate
The experimental conditions were the same as those described in the legend to Fig. 8.

Reaction mixture	Relative free radical generation ^a
Cells only	0.4 ± 0.28
Cells + vanadate	1.5 ± 0.21
Cells + vanadate + superoxide dismutase	3.2 ± 0.42
Cells + vanadate + catalase	0.5 ± 0.35
Cells + vanadate + formate	0.7 ± 0.28
Cells + vanadate + NADPH	3.3 ± 0.56
Cells + vanadate + DPI	0.8 ± 0.28
Cells + vanadate + rotenone	1.0 ± 0.35

^a Data are presented as mean ± S.E. (n = 3).

levels. These results suggest that PI3K activity was required for the HIF-1α expression induced by vanadate. We also investigated whether mitogen-activated protein kinase activity was required for HIF-1α expression induced by vanadate. Cells were pretreated with various concentrations of PD98059, an inhibitor of MAP kinase kinase (MEK). Cells were then treated with 100 μM vanadate for 6 h. As shown in Fig. 2C, addition of PD98059 did not inhibit HIF-1α expression induced by vanadate. These results suggest that MEK activity was not required for HIF-1α expression induced by vanadate.

Induction of PI3K Activity and Akt Phosphorylation by Vanadate—To further confirm that the PI3K activity was involved in HIF-1α expression induced by vanadate, DU145 cells were cultured in MEM supplemented with 10% FBS for 24 h at 37 °C in a 5% CO₂ incubator, followed by treatment with various concentrations of vanadate for 2 h or 100 μM vanadate for various periods as indicated (Fig. 3). The cells were then washed with cold 1× PBS and the total cellular protein extracts (400 μg) were used for determining PI3K activity. As shown in Fig. 3A, PI3K activity was induced by vanadate in a dose-dependent manner. The maximum induction of PI3K activity appeared at 100 μM vanadate. To determine the kinetics of PI3K activity induced by vanadate, the cells were treated

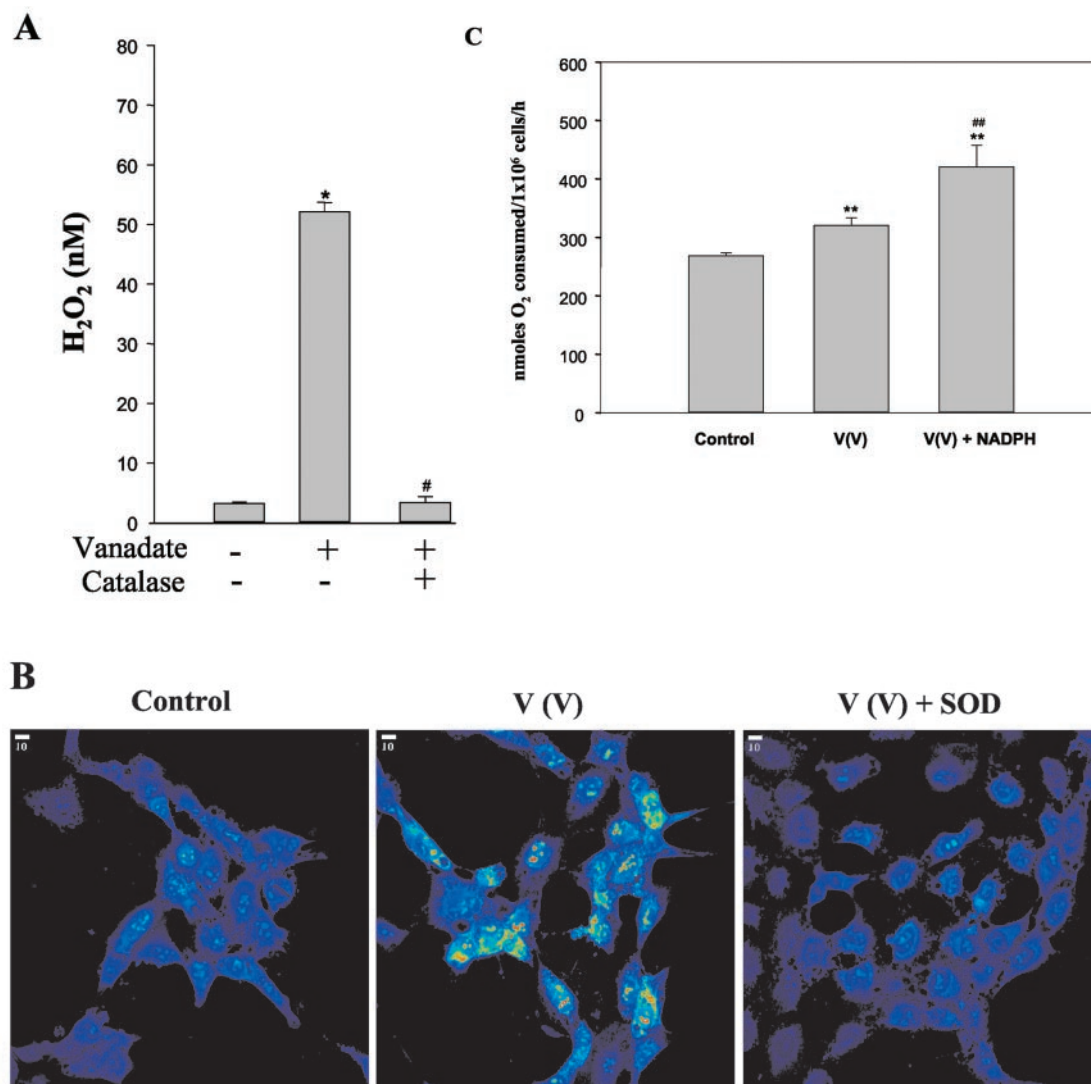


FIG. 9. Analysis of ROS generation. *A*, determination of H₂O₂ by the quantitative H₂O₂ assay kit. 0.1 ml of cell suspension (1×10^6 cells/ml) was incubated with or without vanadate and catalase as indicated, and then mixed with 1.0 ml of working reagent containing 2.5 mM ammonium iron sulfate, 100 mM sorbitol, and 125 μ M xylene orange for 30 min. The absorbance was measured at 560 nm. Values are mean \pm S.E. ($n = 3$). * indicates a significant increase from control, whereas # indicates a significant decrease compared with the vanadate-treated group ($p < 0.01$). *B*, determination of O₂ by HE staining using confocal fluorescence microscopy. The cells were plated onto a glass coverslip in the 12-well plate at 1×10^5 cells/well 24 h before treatment. HE was added into the cell culture 30 min before treatment was completed. After being stained, the cells were washed twice with PBS and fixed with 10% buffered formalin. The images were captured with a confocal fluorescence microscope. *C*, oxygen consumption measurement. DU145 cells were incubated without or with 1 mM vanadate(V) and NADPH. Oxygen consumption was measured with a Gilson oxygraph equipped with a Clark microelectrode as described under "Materials and Methods." Values are mean \pm S.E. ($n = 3$). The double asterisk (**) indicates a significant increase compared with the control without vanadate treatment ($p < 0.01$). ## indicates a significant increase from the vanadate-treated sample ($p < 0.01$).

with 100 μ M vanadate for various times. PI3K activity was induced 5 min, 15 min, 30 min, 1 h, and 2 h after the addition of vanadate (Fig. 3B).

We also investigated endogenous Akt phosphorylation in response to vanadate treatment. Cells were incubated with certain concentrations of vanadate for 2 h, and the total cellular protein extracts were used to determine levels of phospho-Akt for Ser473 and Akt proteins using immunoblot assay. As shown in Fig. 3C, vanadate induced Akt phosphorylation in a dose-dependent manner, whereas it did not alter the Akt protein level. The induction of Akt phosphorylation was maximum by the treatment of vanadate at 100 μ M. To study the kinetics on Akt phosphorylation induced by vanadate, cells were treated with 100 μ M vanadate for 0–4 h, and total cellular protein extracts were used for the assay of phospho-Akt (Ser473) and Akt protein levels. As shown in Fig. 3D, vanadate induced Akt phosphorylation in a time-dependent manner,

whereas it did not affect Akt protein level. The maximum induction of Akt phosphorylation occurred 2 h after the addition of vanadate. These results suggest that vanadate-induced PI3K activity and Akt phosphorylation, and further confirmed that PI3K/Akt pathway was required for vanadate-induced HIF-1 α expression.

Effect of PI3K Inhibitors on Vanadate-induced PI3K Activity and Akt Phosphorylation—To further investigate whether vanadate-induced HIF-1 α expression through the PI3K/Akt pathway, DU145 cells were cultured in MEM supplemented with 10% FBS for 24 h, followed by the addition of LY294002 and wortmannin, respectively, 30 min prior to treatment with 100 μ M vanadate for 2 h. Cellular protein extracts were used for analysis of PI3K activity and Akt phosphorylation. As shown in Fig. 4A, both LY294002 and wortmannin inhibited PI3K activity induced by vanadate. Similarly, these PI3K inhibitors also inhibited the phosphorylation of Akt at Ser473 induced by

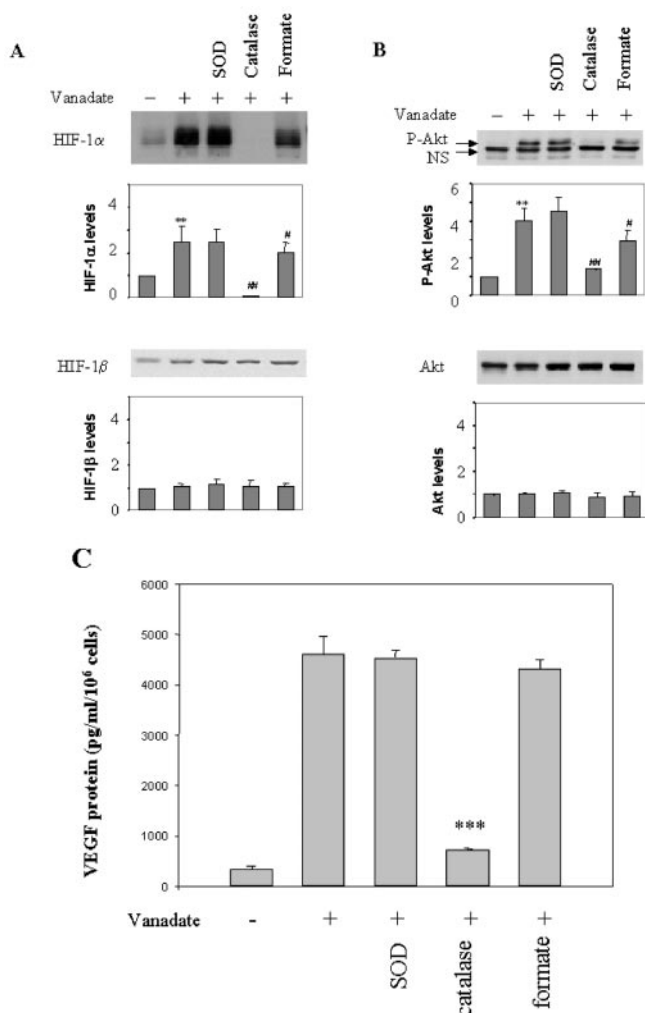


FIG. 10. Effects of antioxidants on vanadate-induced HIF-1 expression, Akt phosphorylation, and VEGF protein secretion. DU145 cells were cultured in MEM supplemented with 10% FBS for 24 h at 37 °C in a 5% CO₂ incubator, followed by pretreatment with various antioxidants for 30 min. Cells were then incubated with 100 μM vanadate for 6 (A) and 2 (B) h. Whole cell extracts were prepared and subjected to immunoblot assay with antibodies against HIF-1α and HIF-1β (A), and phospho-Akt (Ser473) and Akt (B). C, the cells were seeded in a 6-well plate at a density of 1 × 10⁶ cells/well in MEM supplemented with 10% FBS and incubated for 24 h at 37 °C in 5% CO₂, followed by incubation with antioxidants for 30 min prior to the treatment with 50 μM vanadate for 24 h, VEGF protein concentrations in the cell culture media were determined by ELISA (C). The results represent the mean values of VEGF concentration from three separate experiments and duplicate samples of each experiment. Mean ± S.E. values are plotted: **, *p* < 0.01 compared with the control; # and ##, *p* < 0.05 and *p* < 0.01, respectively, compared with the values from the cells treated by vanadate in the absence of the antioxidants. ***, *p* < 0.01 compared with the vanadate-treated group. SOD, superoxide dismutase.

vanadate (Fig. 4, B and C), suggesting that vanadate-induced Akt phosphorylation was through PI3K activation, and further confirming that the PI3K/Akt pathway was required for induction of HIF-1α expression induced by vanadate.

Role of mTOR/FRAP in HIF-1 Expression—To investigate whether rapamycin, a mTOR/FRAP inhibitor, could inhibit HIF-1α expression induced by vanadate, DU145 cells were cultured in MEM supplemented with 10% FBS for 24 h, followed by the addition of rapamycin 30 min prior to the treatment of 100 μM vanadate for 6 h. Cellular lysates were prepared and used to determine HIF-1α and HIF-1β protein levels. As shown in Fig. 5, rapamycin inhibited vanadate-induced

HIF-1α expression in a dose-dependent manner, whereas rapamycin did not cause any decrease in HIF-1β protein level. The results suggest that mTOR/FRAP, a downstream target of PI3K/Akt, was required for HIF-1α expression induced by vanadate.

Induction of VEGF Expression—HIF-1 is known to activate VEGF expression in response to low oxygen. To investigate whether induction of HIF-1α expression by vanadate results in an increase in HIF-1-regulated gene expression, the level of VEGF protein in DU145 cells after exposure of vanadate was analyzed using ELISA. Treatment of cells with 50 μM vanadate significantly increased VEGF levels in a time-dependent manner, when compared with VEGF levels in untreated cells (Fig. 6).

Effect of PI3K Inhibitors and MAP Kinase Kinase Inhibitor on VEGF Expression—To investigate whether PI3K and MEK were involved in the expression of VEGF, DU145 cells were cultured in MEM supplemented with 10% FBS for 24 h, followed by the addition of PI3K inhibitors, LY294002 and wortmannin, or the MEK inhibitor, PD98059, 30 min prior to the treatment of vanadate. Cells were then treated with 50 μM vanadate for 24 h. VEGF protein concentration in the media was determined by ELISA. As shown in Fig. 7, LY294002 and wortmannin significantly decreased the VEGF protein levels induced by vanadate, whereas MEK inhibitor, PD98059, did not exhibit any inhibitory effect. These results further suggest that PI3K signaling was required for induction of HIF-1α and VEGF expression induced by vanadate, whereas MEK activity was not required.

Requirement of ROS for Induction of HIF-1α Expression—ROS are known to play a major role in vanadate-induced carcinogenesis (44, 45). To determine whether vanadate could induce HIF-1α expression through ROS, we first examined the ROS generation in the vanadate-treated cells. The ability of vanadate to generate ·OH radicals was examined using an ESR spin trapping method with DMPO as the spin trap. DU145 cells alone exhibited a weak ESR signal from the impurity in the spin trap, but did not produce any detectable amount of free radicals (Fig. 8A). The cells incubated with vanadate generated a typical ESR spectrum because of cellular reduction of vanadate in phosphate-buffered solution (pH 7.4) (Fig. 8B). The spectrum consists of a 1:2:2:1 quartet with a splitting of $a_H = a_N = 14.9$ G, where a_N and a_H denote the hyperfine splitting of the nitroxyl nitrogen and α-hydrogen, respectively. Based on these splittings and the 1:2:2:1 line shape, this spectrum was assigned to the DMPO/·OH adduct, which was evidence of ·OH radical generation. Addition of superoxide dismutase, a O₂⁻ scavenger whose function was to convert O₂⁻ to H₂O₂, markedly increased the DMPO/·OH adduct signal (Fig. 8C). Catalase, an H₂O₂ scavenger, decreased the generation of ·OH radical (Fig. 8D); sodium formate, a scavenger of ·OH radical, also decreased the intensity of the DMPO/·OH signal (Fig. 8E). NADPH, a cofactor of certain flavoenzymes such as glutathione reductase, which catalyzes the reduction of vanadate to vanadium(IV), markedly enhanced the generation of the ·OH radical (Fig. 8F). To determine whether NADPH oxidase or the mitochondria electron transport chain could play an important role in vanadate-induced ROS generation, DPI, a NADPH oxidase inhibitor, and rotenone, a mitochondria electron transport inter-rupter, were used. As shown in Fig. 8, G and H, both DPI and rotenone reduced ·OH radical generation induced by vanadate. The data were similar in three independent experiments (Table I). These results indicated that both NADPH oxidase and mitochondria electron transport chain contributed to vanadate(V)-induced ROS generation.

The ability of vanadate to generate H₂O₂ in DU145 cells was

analyzed by a quantitative H_2O_2 assay kit. In the presence of vanadate, H_2O_2 was dramatically enhanced compared with control, whereas catalase, an H_2O_2 scavenger, markedly suppressed the formation of H_2O_2 (Fig. 9A).

A specific fluorescent dye was used to visualize free radical generation directly inside the DU145 cells. HE, a specific fluorescent dye for O_2^- , was used to detect the generation of O_2^- . The cells were visualized with a laser scanning confocal microscope (Fig. 9B). Because this oxygen species was mainly produced in the mitochondria, the bright color fluorescent dots in the cytoplasm represent the subcellular location of the O_2^- (Fig. 9B). Compared with control, vanadate treatment enhanced O_2^- radical production, whereas addition of superoxide dismutase suppressed its production to basal level (Fig. 9B). HE exhibits a red or orange color after being oxidized by O_2^- . Because O_2^- was the one-electron reduction product of molecular oxygen, the O_2 consumption in cells treated with vanadate was measured using a Gilson oxygraph equipped with a Clark electrode. As shown in Fig. 9C, vanadate increased O_2 consumption, and addition of NADPH further enhanced it.

Involvement of ROS in HIF-1 α and VEGF Expression and Akt Phosphorylation—To understand whether ROS generated by vanadate in DU145 play a role in vanadate-induced HIF-1 α expression through the PI3K pathway, the effects of various antioxidants on vanadate-induced HIF-1 α expression and Akt phosphorylation were determined using immunoblot assay. As shown in Fig. 10, A and B, treatment of the cells with 100 μ M vanadate induced HIF-1 α expression and Akt phosphorylation. Catalase, an H_2O_2 scavenger, inhibited both vanadate-induced HIF-1 α expression and Akt phosphorylation. Sodium formate, a \cdot OH radical scavenger, slightly inhibited HIF-1 α expression and Akt phosphorylation. In contrast, treatment of cells with superoxide dismutase did not inhibit HIF-1 α expression or Akt phosphorylation. To further study the role of ROS in HIF-1-regulated gene expression, the effects of various specific antioxidants on vanadate-induced VEGF expression were determined using ELISA. As shown in Fig. 10C, treatment of cells with vanadate increased VEGF protein levels, and addition of catalase significantly inhibited VEGF expression. Sodium formate did not significantly affect the VEGF level, which may be because of the decrease of HIF-1 expression (Fig. 10A). In contrast, treatment of cells with superoxide dismutase did not significantly inhibit the VEGF expression induced by vanadate.

DISCUSSION

The results obtained from this study show that vanadate was able to induce HIF-1 α and VEGF protein expression in a dose- and time-dependent manner in DU145 cells, whereas HIF-1 β protein expression was not affected by vanadate treatment. It has been reported that HIF-1 β is not significantly affected by cellular oxygen tension (3). HIF-1 α protein is rapidly degraded under normoxic condition by the ubiquitin-proteasome system (54, 55), whereas hypoxia and $CoCl_2$ (56, 57) induce both the stabilization and the transactivation of HIF-1 α (34, 35). It has also been reported that insulin, like hypoxia, induces HIF-1 α expression (46–49). Because vanadium has been found to act in an insulin-like manner, vanadate may increase HIF-1 α expression by a similar signal pathway as insulin and hypoxia. It is known that HIF-1 activates VEGF expression by directly binding to VEGF promoter in response to hypoxia (2, 3, 58). Similarly, the induction of HIF-1 by vanadate resulted in an increased level of VEGF expression. There is a strong correlation between VEGF expression and cancer progression and metastasis (22). Inhibition of VEGF expression has a dramatic effect on tumor growth, invasion, and metastasis (24, 25, 59–66). It is

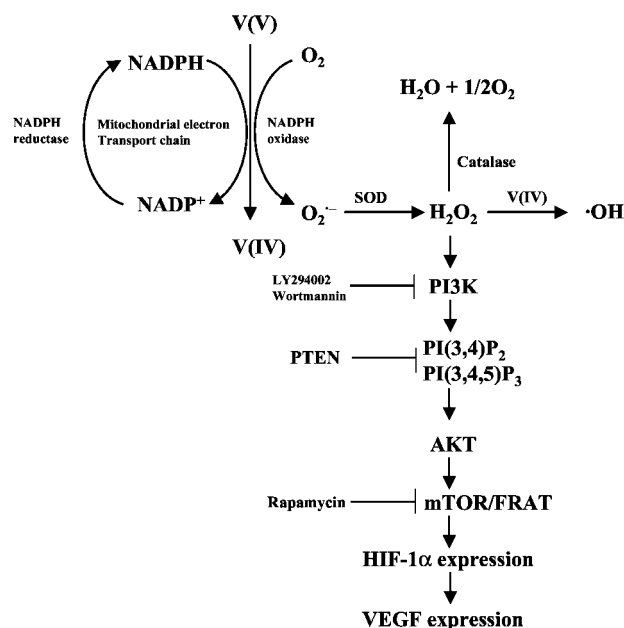


FIG. 11. Schematic representation of possible mechanism of vanadate-induced HIF-1 and VEGF expression.

possible that the induction of HIF-1 and VEGF may play an important role in vanadate-induced carcinogenesis.

The present study also indicates that the PI3K/AKT/FRAP signaling pathway was required for induction of HIF-1 and VEGF expression induced by vanadate, whereas the mitogen-activated protein kinase/ERK pathway was not involved. The following results provide the evidence to support this conclusion: (a) PI3K inhibitors, LY294002 and wortmannin, inhibited HIF-1 α expression induced by vanadate, whereas MEK inhibitor, PD98059, did not; (b) vanadate-induced PI3K activity in a dose- and time-dependent manner, and LY294002 and wortmannin inhibited the vanadate-induced PI3K activity; (c) vanadate induced Akt phosphorylation in a dose- and time-dependent manner, and LY294002 and wortmannin inhibited the Akt phosphorylation; (d) rapamycin, a mTOR/FRAP inhibitor, inhibited HIF-1 α expression induced by vanadate in a dose-dependent manner; and (e) LY294002 and wortmannin decreased the VEGF protein level induced by vanadate in a dose-dependent manner, whereas the MEK inhibitor, PD98059, did not exhibit any effect. These data suggest that activation of the PI3K/AKT/mTOR signaling pathway and induction of HIF-1 and VEGF expression could be an important mechanism to understand the vanadate-induced carcinogenesis.

Our study also indicates that ROS are involved in vanadate-induced HIF-1 α and VEGF expression. Among them, H_2O_2 plays a critical role based on the following evidence: (a) exposure of cells to vanadate-generated H_2O_2 as determined by quantitative H_2O_2 assay; (b) ESR spin trapping measurements show that cells pretreated with vanadate generated \cdot OH radical using H_2O_2 as a precursor; (c) vanadate increased the rate of cellular oxygen consumption; (d) catalase, a specific scavenger of H_2O_2 , decreased the generation of ROS induced by vanadate; (e) catalase inhibited HIF-1 α and VEGF expression and Akt phosphorylation induced by vanadate, whereas sodium formate, a scavenger of \cdot OH, showed a minor effect; and (f) superoxide dismutase, a scavenger of O_2^- , did not inhibit vanadate-induced HIF-1 α and VEGF expression or AKT phosphorylation. It may be noted that catalase, a scavenger of H_2O_2 , abolished the hypoxia- and $CoCl_2$ -induced stabilization of HIF-1 α , and exogenous H_2O_2 stabilized HIF-1 α expression during normoxia, suggesting that H_2O_2 acts as a signaling

element in this response (64). The mechanism of ROS generation induced by vanadate could be that in the presence of NADPH and several cellular flavoenzymes (such as glutathione reductase, lipoyl dehydrogenase, ferredoxin-NADP⁺, and NADPH oxidase) the mitochondria electron transport chain is able to reduce vanadate to vanadium(IV) (44). During the reduction process, molecular oxygen was consumed to generate O₂^{•-}, which was subsequently converted to H₂O₂ through superoxide dismutase dismutation (Fig. 11). Vanadium(IV) is also able to generate •OH radical from H₂O₂ via a Fenton-like reaction (44, 52, 64).

Molecular oxygen is the original source of ROS generation in DU145 cells under vanadate stimulation as demonstrated by the oxygen consumption assay. The major pathways involved in ROS generation are both the flavoprotein-containing NADPH oxidase complex and the mitochondrial electron transport chain. This conclusion is supported by the inhibition of ROS generation by DPI, a flavoprotein inhibitor, as well as rotenone, an inhibitor of the mitochondrial electron chain as determined by ESR measurements. In conclusion, this work demonstrates that vanadate is able to induce HIF-1 α and VEGF expression via the PI3K/AKT/mTOR/FRAP signaling pathway. H₂O₂ generated during the cellular reduction of vanadate is the major species responsible for vanadate-induced expression of HIF-1 α and VEGF. Further study of the role of HIF-1 α and VEGF expression in vanadate-induced carcinogenesis will be the next important challenge.

REFERENCES

- Jiang, B. H., Rue, E., Wang, G. L., Roe, R., and Semenza, G. L. (1996) *J. Biol. Chem.* **271**, 17771–17778
- Wang, G. L., Jiang, B. H., Rue, E. A., and Semenza, G. L. (1995) *Proc. Natl. Acad. Sci. U. S. A.* **92**, 5510–5514
- Jiang, B. H., Semenza, G. L., Bauer, C., and Marti, H. H. (1996) *Am. J. Physiol.* **271**, C1172–C1180
- Hoffman, E. C., Reyes, H., Chu, F. F., Sander, F., Conley, L. H., Brooks, B. A., and Hankinson, O. (1991) *Science* **252**, 954–958
- Forsythe, J. A., Jiang, B. H., Iyer, N. V., Agani, F., Leung, S. W., Koos, R. D., and Semenza, G. L. (1996) *Mol. Cell. Biol.* **16**, 4604–4613
- Lee, P. J., Jiang, B. H., Chin, B. Y., Iyer, N. V., Alam, J., Semenza, G. L., and Choi, A. M. (1997) *J. Biol. Chem.* **272**, 5375–5381
- Semenza, G. L., Jiang, B. H., Leung, S. W., Passantino, R., Concorde, J. P., Maire, P., and Giallongo, A. (1996) *J. Biol. Chem.* **271**, 32529–32537
- Semenza, G. L., Agani, F., Booth, G., Forsythe, J., Iyer, N., Jiang, B. H., Leung, S., Roe, R., Wiener, C., and Yu, A. (1997) *Kidney Int.* **51**, 553–555
- Jiang, B. H., Agani, F., Passaniti, A., and Semenza, G. L. (1997) *Cancer Res.* **57**, 5328–5335
- Maxwell, P. H., Dachs, G. U., Gleadle, J. M., Nicholls, L. G., Harris, A. L., Stratford, I. J., Hankinson, O., Pugh, C. W., and Ratcliffe, P. J. (1997) *Proc. Natl. Acad. Sci. U. S. A.* **94**, 8104–8109
- Mazure, N. M., Chen, E. Y., Laderoute, K. R., and Giaccia, A. J. (1997) *Blood* **90**, 3322–3331
- Zhong, H., De Marzo, A. M., Laughner, E., Lim, M., Hilton, D. A., Zagzag, D., Buechler, P., Isaacs, W. B., Semenza, G. L., and Simons, J. W. (1999) *Cancer Res.* **59**, 5830–5835
- Jiang, B. H., Jiang, G., Zheng, J. Z., Lu, Z., Hunter, T., and Vogt, P. K. (2001) *Cell Growth Differ.* **12**, 363–369
- Minet, E., Arnould, T., Michel, G., Roland, I., Mottet, D., Raes, M., Remacle, J., and Michiels, C. (2000) *FEBS Lett.* **468**, 53–58
- Richard, D. E., Berra, E., Gothie, E., Roux, D., and Pouyssegur, J. (1999) *J. Biol. Chem.* **274**, 32631–32637
- Zhong, H., Chiles, K., Feldser, D., Laughner, E., Hanrahan, C., Georgescu, M. M., Simons, J. W., and Semenza, G. L. (2000) *Cancer Res.* **60**, 1541–1545
- Maxwell, P. H., Wiesener, M. S., Chang, G. W., Clifford, S. C., Vaux, E. C., Cockman, M. E., Wykoff, C. C., Pugh, C. W., Maher, E. R., and Ratcliffe, P. J. (1999) *Nature* **399**, 271–275
- Cockman, M. E., Masson, N., Mole, D. R., Jaakkola, P., Chang, G. W., Clifford, S. C., Maher, E. R., Pugh, C. W., Ratcliffe, P. J., and Maxwell, P. H. (2000) *J. Biol. Chem.* **275**, 25733–25741
- Kamura, T., Sato, S., Iwai, K., Czyzyk-Krzeska, M., Conaway, R. C., and Conaway, J. W. (2000) *Proc. Natl. Acad. Sci. U. S. A.* **97**, 10430–10435
- Ohh, M., Park, C. W., Ivan, M., Hoffman, M. A., Kim, T. Y., Huang, L. E., Pavletich, N., Chau, V., and Kaelin, W. G. (2000) *Nat. Cell Biol.* **2**, 423–427
- Tanimoto, K., Makino, Y., Pereira, T., and Poellinger, L. (2000) *EMBO J.* **19**, 4298–4309
- Bruick, R. K., and McKnight, S. L. (2001) *Science* **294**, 1337–1340
- Jaakkola, P., Mole, D. R., Tian, Y. M., Wilson, M. I., Gielbert, J., Gaskell, S. J., Kriegsheim, A., Hebestreit, H. F., Mukherji, M., Schofield, C. J., Maxwell, P. H., Pugh, C. W., and Ratcliffe, P. J. (2001) *Science* **292**, 468–472
- Masson, N., Willam, C., Maxwell, P. H., Pugh, C. W., and Ratcliffe, P. J. (2001) *EMBO J.* **20**, 5197–5206
- Liu, Y., Cox, S. R., Morita, T., and Kourembanas, S. (1995) *Circ. Res.* **77**, 638–643
- Ferrara, N., and Davis-Smyth, T. (1997) *Endocr. Rev.* **18**, 4–25
- Millauer, B., Longhi, M. P., Plate, K. H., Shawver, L. K., Risau, W., Ullrich, A., and Strawn, L. M. (1996) *Cancer Res.* **56**, 1615–1620
- Plate, K. H., Breier, G., Weich, H. A., and Risau, W. (1992) *Nature* **359**, 845–848
- Plate, K. H., Breier, G., Millauer, B., Ullrich, A., and Risau, W. (1993) *Cancer Res.* **53**, 5822–5827
- Strawn, L. M., McMahon, G., App, H., Schreck, R., Kuchler, W. R., Longhi, M. P., Hui, T. H., Tang, C., Levitzki, A., Gazit, A., Chen, I., Kerl, G., Orfi, L., Risau, W., Flamme, I., Ullrich, A., Hirth, K. P., and Shawver, L. K. (1996) *Cancer Res.* **56**, 3540–3545
- Crans, D. C., Simone, C. M., Saha, A. K., and Glew, R. H. (1989) *Biochem. Biophys. Res. Commun.* **165**, 246–250
- Nriagu, J. O., and Pacyna, J. M. (1988) *Nature* **333**, 134–139
- Rojas, E., Herrera, L. A., Porier, L. A., and Ostrosky-Wegman, P. (1999) *Mutat. Res.* **443**, 157–181
- Stock, P. (1960) *Br. J. Cancer* **14**, 397–418
- Hickey, R. J., Schoff, E. P., and Clelland, R. C. (1967) *Arch. Environ. Health* **15**, 728–738
- Kraus, T., Raithe, H., and Schaller, K. H. (1989) *Zentralbl. Hyg. Umweltmed.* **188**, 108–126
- Altamirano-Lozano, M., Alvarez-Barrera, L., Basurto-Alcantara, F., Valverde, M., and Rojas, E. (1996) *Teratog. Carcinog. Mutagen.* **16**, 7–17
- Rojas, E., Valverde, M., Altamirano-Lozano, M., and Ostrosky-Wegman, P. (1996) *Mutat. Res.* **359**, 77–84
- Roldan, R. E., and Altamirano, L. M. A. (1990) *Mutat. Res.* **245**, 61–65
- Sabbioni, E., Pozzi, G., Pintar, A., Casella, L., and Garattini, S. (1991) *Carcinogenesis* **12**, 47–52
- Sheu, C. W., Rodriguez, I., and Leet, J. K. (1992) *Food Chem. Toxicol.* **30**, 307–311
- Sabbioni, E., Pozzi, G., Devos, S., Pintar, A., Casella, L., and Fischbach, M. (1993) *Carcinogenesis* **14**, 2565–2568
- Kerckaert, G. A., LeBoeuf, R. A., and Isfort, R. J. (1996) *Fundam. Appl. Toxicol.* **34**, 67–72
- Ding, M., Li, J. J., Leonard, S. S., Ye, J., Shi, X., Colburn, N. H., Castranova, V., and Vallyathan, V. (1999) *Carcinogenesis* **20**, 663–668
- Ye, J., Ding, M., Leonard, S. S., Robinson, V. A., Michecchia, L., Zhang, X., Castranova, V., Vallyathan, V., and Shi, X. (1999) *Mol. Cell. Biochem.* **202**, 9–17
- Goldwasser, I., Gefel, D., Gershonov, E., Fridkin, M., and Shechter, Y. (2000) *J. Inorg. Biochem.* **80**, 21–25
- Barbagallo, M., Dominguez, L. J., and Resnick, L. M. (2001) *Hypertension* **38**, 701–704
- Minet, E., Michel, G., Remade, J., and Michiels, C. (2000) *Int. J. Mol. Med.* **5**, 253–259
- Zelzer, E., Levy, Y., Kahana, C., Shilo, B. Z., Rubinstein, M., and Cohen, B. (1998) *EMBO J.* **17**, 5085–5094
- Rosen, G. M., and Finkelstein, E. (1985) *Adv. Free Radical Biol. Med.* **1**, 345–375
- Shi, X., and Dalal, N. S. (1992) *Free Radical Res. Commun.* **17**, 369–376
- Shi, X., and Dalal, N. S. (1991) *Arch. Biochem. Biophys.* **289**, 355–361
- Marchetti, P., Castedo, M., Susin, S. A., Zamzami, N., Hirsch, T., Macho, A., Haefliger, A., Hirsch, F., Geuskens, M., and Kroemer, G. (1996) *J. Exp. Med.* **184**, 1155–1160
- Huang, L. E., Gu, J., Schau, M., and Bunn, H. F. (1998) *Proc. Natl. Acad. Sci. U. S. A.* **95**, 7987–7992
- Kallio, P. J., Wilson, W. J., O'Brien, S., Makino, Y., and Poellinger, L. (1999) *J. Biol. Chem.* **274**, 6519–6525
- Salceda, S., and Caro, J. (1997) *J. Biol. Chem.* **272**, 22642–22647
- Sandau, K. B., Fandrey, J., and Brune, B. (2001) *Blood* **97**, 1009–1015
- Gong, P., Hu, B., Stewart, D., Ellerbe, M., Figueroa, Y. G., Blank, V., Beckman, B. S., and Alam, J. (2001) *J. Biol. Chem.* **276**, 27018–27025
- Kotch, L. E., Iyer, N. V., Laughner, E., and Semenza, G. L. (1999) *Dev. Biol.* **209**, 254–267
- Benjamin, L. E., and Keshet, E. (1997) *Proc. Natl. Acad. Sci. U. S. A.* **94**, 8761–8766
- Borgstrom, P., Hillan, K. J., Sriramarao, P., and Ferrara, N. (1996) *Cancer Res.* **56**, 4032–4039
- Cheng, S.-Y., Huang, H.-J. S., Nagane, M., Ji, X.-D., Wang, D., Shih, C. C.-Y., Arap, W., Huang, C.-M., and Cavenee, W. K. (1996) *Proc. Natl. Acad. Sci. U. S. A.* **93**, 8502–8507
- Grunstein, J., Roberts, W. G., Mathieu-Costello, O., Hanahan, D., and Johnson, R. S. (1999) *Cancer Res.* **59**, 1592–1598
- Shi, X. L., Sun, X. Y., and Dalal, N. S. (1990) *FEBS Lett.* **271**, 185–188